Journal of ELECTRONIC MATERIALS, Vol. 37, No. 5, 2008
DOI: 10.1007/s11664-007-0295-1

Special Issue Paper

First-Principles Studies of Metal (111)/ZnO{0001} Interfaces

YUFENG DONG[1,2] and L.J. BRILLSON[1]

1.—Department of Electrical and Computer Engineering, The Ohio State University, Columbus, OH 43210, USA. 2.—e-mail: dong.70@osu.edu

The atomic and electronic structures for various metal (111)/ZnO{111} interfaces were studied by first-principles calculations based on density functional theory. The Schottky barrier heights (SBHs) were evaluated for Al, Ag, and Au/ZnO interfaces. SBHs at metal/ZnO polar interfaces were found to be very sensitive to the specific interface chemical bonding. Interface metal-zinc bonding tends to give Ohmic contacts, while the contribution of metal-oxygen bonds depends on the specific metal: simple metals gives Ohmic contacts whereas noble metals gives Schottky-like behavior. We discussed the implications of these results for controlling the formation of metal/ZnO contacts.

Key words: ZnO, first principles, metal/ZnO interface, Schottky barrier height

INTRODUCTION

ZnO is attracting intensive interest as an important candidate for next-generation semiconductor electronics.[1] Metal/ZnO interfaces are central to all ZnO electronic device applications, yet their electronic properties have only recently been explored in detail.[2–4] It has been shown that all the measured barrier heights are lower than the predicted Schottky–Mott values and do not vary in proportion to the difference in the work function values.[5] The failure of the Schottky–Mott theory to predict the Schottky barrier heights (SBHs) indicates that interface features such as surface contamination,[3] interface native defects,[6,7] chemical bonding[8,9] or other extrinsic factors,[10] play a very important role. It has recently been shown that surface conditions and near-surface native defects can affect ZnO SBHs.[6] However, these *n*-type barriers generally appear limited to 0.6–0.8 eV even after surface and subsurface defects of ZnO substrate are minimized, e.g., by O_2/He plasma treatment. This motivates us to identify the effects of other interface features, besides the surface contamination and interface defects, on the ZnO SBHs, so that the formation mechanism at metal/ZnO interfaces can be fully understood. It has been found for many metal/semiconductor contacts that SBHs depend on interface chemical bonding.[11–14] Recent theoretical studies describe preferred adsorption sites for several metals on ZnO surfaces;[15–17] however, the atomic and electronic structures of metals on the ZnO surfaces and their relation to the SBH remain unknown. In this paper, we report a study of the atomic and electronic structures of various metal (111)/ZnO{0001} interfaces. The effects of interface chemical bonding on ZnO SBHs were also evaluated.

The calculations presented in this paper highlight the influence of local chemical bonding at clean, ordered metal–semiconductor interfaces that are free of lattice defects or interfacial layers. These calculations reveal the fact that, even under such idealized conditions, the local bonding between metal and semiconductor can produce a significant effect on Schottky barrier heights due to the interfacial dipole contribution they make. Extrinsic effects such as impurities, defects, or interfacial layers comprised of elements besides those of the metal and semiconductor can introduce substantial differences—as many studies of Schottky barriers have directly (or sometimes unintentionally) attested to.

(Received June 8, 2007; accepted September 4, 2007; published online October 2, 2007)

METHODS AND PROCEDURE

Our first-principles methods are based on density functional theory (DFT) within the general gradient approximation (GGA). The calculations were performed using the Vienna *ab initio* simulation package (VASP)[18] with the frozen-core projector-augmented-wave (PAW) pseudopotentials.[19] We use a plane-wave cut off corresponding to a kinetic energy of 400 eV, a $9 \times 9 \times 9$ **k**-point mesh for the wurtzite primitive ZnO cell and a $9 \times 9 \times 1$ **k**-point mesh for metal (111)/ZnO{0001} interface supercells. It is well known that GGA-DFT underestimates the binding energy of the Zn *d* states and predicts a very low band gap (0.6–0.8 eV versus 3.4 eV experimental value) for ZnO. Here, we include the on-site Coulomb correction for the Zn *d* states, the so called GGA + U method,[20] which can partially correct the enlarged O–*p* and Zn–*d* coupling and improve the prediction of the band gap.

Table I shows the calculated lattice constants and band gap. The structural lattice parameters are in good agreement with that of experiments and other theoretical studies.[21] The GGA + U method increases the band gap to 1.82 eV, which is very close to that in a recent GGA + U calculation.[22] Although this value is still much lower than the experimental one, it opens up the window for the variation of metal Fermi levels within the band gap of ZnO compared to conventional GGA and is beneficial for the study of metal/ZnO interfaces. The atom projected density of states (PDOS) for ZnO from GGA and GGA + U is shown in Fig. 1. The states at the valence band edge are mainly derived from O 2p, while Zn 3d electrons are mainly localized around 5.3 eV and 7.2 eV below the valence band edge for GGA and GGA + U, respectively. The Zn–O bond is partially ionic with covalent character due to the hybridization of O 2p and Zn 3d states. With self-interaction corrections included, the localized Zn 3d states are well separated from the upper valence bands and the band gap increases significantly.

The metal/ZnO interface structure is very complicated even for abrupt, defect-free interfaces. Here, we consider metal (111) and ZnO{0001} surfaces as the building blocks. Perpendicular to the ZnO *c* axis, there are two kinds of polar surfaces: O-terminated $(000\bar{1})$ and Zn-terminated (0001). Because there is no mirror symmetry parallel to the polar surfaces, a ZnO{0001} surface slab is always O terminated on one side and Zn terminated on the other. Three different high-symmetry adsorption sites were considered: on top, hcp hollow, and fcc hollow, as shown in Fig. 2. It has been shown that, for an O-terminated surface, metal atoms tend to sit on the top of O, while for a Zn-terminated surface, both hcp and fcc hollow are preferable.[15–17] We will study these three interface structures for the metals Al, Ag, and Au on ZnO.

For fcc metals, Al, Ag, and Au, the in-plane lattice mismatch with ZnO is around 11%. Because metal films are more flexible, we treated ZnO as the substrate and fixed the in-plane lattice constant as that of ZnO. (1×1) interface supercells include nine layers of metal and 14–18 Zn-O double layers. The lattice constant along the interface normal and all the atoms are allowed to relax to minimize the total energy of the supercell. One may wonder what the effects of this artificially imposed strain in the metal

Table I. Lattice Constants *a* (Å) and c/*a*, Internal Structure Parameter *u*, and Band Gap (E_g, eV) of ZnO

	This Work			Ref. 21	
	GGA	GGA + U	Expt.	LDA	LDA + U
a	3.285	3.196	3.249	3.195	3.148
c/*a*	1.605	1.604	1.602	1.615	1.612
u	0.382	0.382	0.382	0.379	0.379
E_g	0.72	1.82	3.43	0.80	1.51

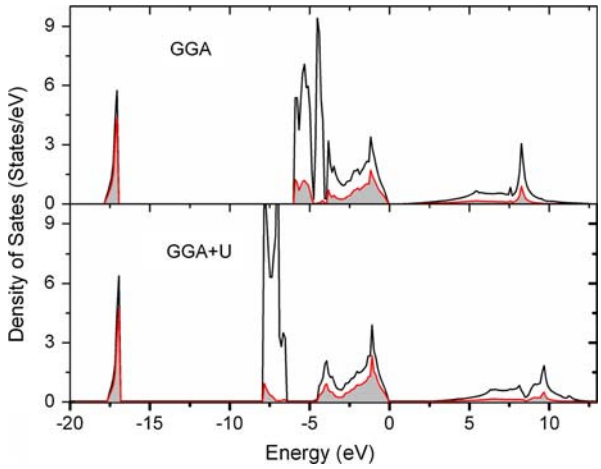

Fig. 1. Total density of states (DOS, open feature) and atom projected density of states (PDOS, for O atom, shaded feature) from GGA and GGA + U. GGA + U increases the calculated band gap. The valence band edge is at energy zero.

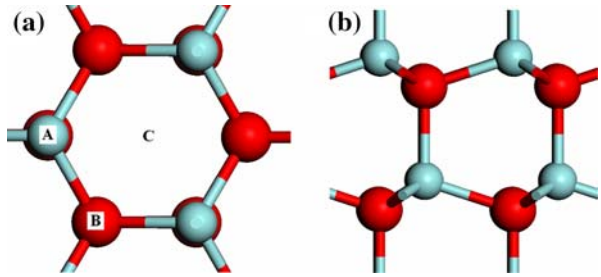

Fig. 2. Top view (a) and side view (b) for high-symmetry adsorption sites on ZnO{0001} surface. A: on top, B: hcp-hollow, and C: fcc-hollow.

Table II. In-plane Lattice Mismatch (with ZnO{0001}, $\Delta a/a$) and Work Function (WF) for Metal (111) under Strain or Unstrained

		WF (eV)		
	$\Delta a/a$ (%)	Strained	Perfect	Expt.
Al	11.8	4.33	4.10	4.28
Ag	11.1	4.23	4.37	4.26
Au	11.2	4.97	5.22	5.10

are. Table II shows the calculated work functions (WFs) for in-plane strained and unstrained (perfect) metal (111) surfaces. Experimental values of metal WFs are also given for reference.[23] The calculated (perfect) WFs are in good agreement with the experimental values (Expt.). With in-plane strain, the WF for Al increases slightly (0.2 eV), while that of Ag and Au decreases (0.1–0.2 eV). Therefore, the variation of WF under strain is not significant and will not change our conclusion in general.

RESULTS AND DISCUSSION

Figure 3 shows the atom projected density of states (PDOS) at Al/ZnO and Au/ZnO interfaces. Both O- and Zn-terminated interfaces are shown. For Zn-terminated interfaces, the hcp and fcc hollow structures are very similar. Only the latter are shown here. The PDOS for atoms at the interface (Int.) are shown in solid lines, while that for Al (Au) atoms in their respective bulk region and ZnO in the second double-layer (2nd) are shown in dotted lines. For the DOS of ZnO in the bulk region, one can also refer to Fig. 1. The most important feature of all the PDOS shown in Fig. 3 is the presence of metal-induced gap states (MIGS) for interface ZnO atoms, as shown by the states in the ZnO band gap region (around the Fermi level). However, the MIGS almost disappear from the second double-layer of ZnO (dotted lines) and ZnO recovers its bulk character quickly from there, which indicates a strong screening of ZnO to the outside metal. One may notice that the Fermi level varies within the band gap of ZnO for different interface structures (O- or Zn-terminated Al- or Au-ZnO interfaces). We would stress here that the position of the interface Fermi level is determined by the interface chemistry (boundary condition) and indicates the variation of SBHs with interface chemical bonding, although SBHs cannot be derived directly here.

The shapes of the PDOS for interface atoms are also modified from their bulk counterparts. For O-terminated interfaces, this is due to the formation of oxygen-metal bonds, while for Zn-terminated interfaces, Zn-metal bonds form. There are bonding peaks in the DOS for the Al-O, Au-Zn, and Au-O interface bonds, while for Al-Zn bonds the DOS for interfacial Al atoms changes little. For the Al/ZnO interface, the Al atom on top of O forms a strong ionic bond with the nearby O atom, as evidenced by the bonding peaks at about –6.3 eV both in Al and O DOS. There is also an energy shift (0.6 eV to higher binding energy) for interface ZnO atoms relative to the second layer of ZnO. This indicates a strong interaction of the surface ZnO atoms with the Al. However, the Al at the Zn-terminated interfaces shows a free-electron-like behavior, close to that in the bulk region. Accordingly, the shapes of the PDOS for interface ZnO atoms were also only modified slightly except for the MIGS. This means a stronger screening in the O-terminated surface for Al/ZnO interface. For Au/ZnO interface, both the DOS of the Au atoms at two polar interfaces (O- and Zn-terminated) change. The former has an energy shift ($\sim$0.5 eV) to lower energy, while the latter becomes narrower and sharper and there is a bonding peak at around –4.1 eV, compared to their bulk counterparts (dotted lines). Correspondingly, bonding peaks form at about –3.9 eV and near the O valence band edge for O PDOS due to the formation of interface O-Au bonding whereas the localized d states of Zn move 0.4 eV to higher binding energy for the formation of Zn-Au interface bonding. This is due to the hybridization of Au 5d states with O 2p and Zn 3d, 4s states at the two interfaces, respectively.

Now we turn to discuss the most important transport parameter for metal/ZnO interfaces, the SBH and its relation with the interface chemical bonding. Normally, the band offsets or SBH can be determined using the standard bulk-plus-lineup method.[24–26] In this method, one reference level (such as the potential, similar to the core level in spirit) is chosen. The energy difference between the valence band edge (E_V) and the reference level is assumed to be a constant for a given material, which can be determined in the bulk calculations. For metal/oxide supercell, the n-type SBH (Φ_B) can be expressed as,

$$\Phi_B = E_g - (E_F - E_V) = E_g - [E_F - (\bar{V} + \Delta)] \quad (1)$$

where E_g is the band gap, E_F is the Fermi level of the interface supercell, $\bar{V}$ is the reference level, the averaged potential in the bulk region of interface supercell, and Δ is the energy difference between the valence band edge (E_V) and the reference level (averaged potential). E_F and $\bar{V}$ are obtained from the interface supercell calculation, while Δ is obtained from the calculation for a wurtzite ZnO primitive cell. One requirement for this bulk-plus-lineup method is that the two parts of the interface should recover their respective bulk properties far away from the interface. This can be satisfied by choosing supercells long enough to minimize the interaction of the two interfaces within the supercell.

However, because the O- and Zn-terminated interfaces are inequivalent but present in the same

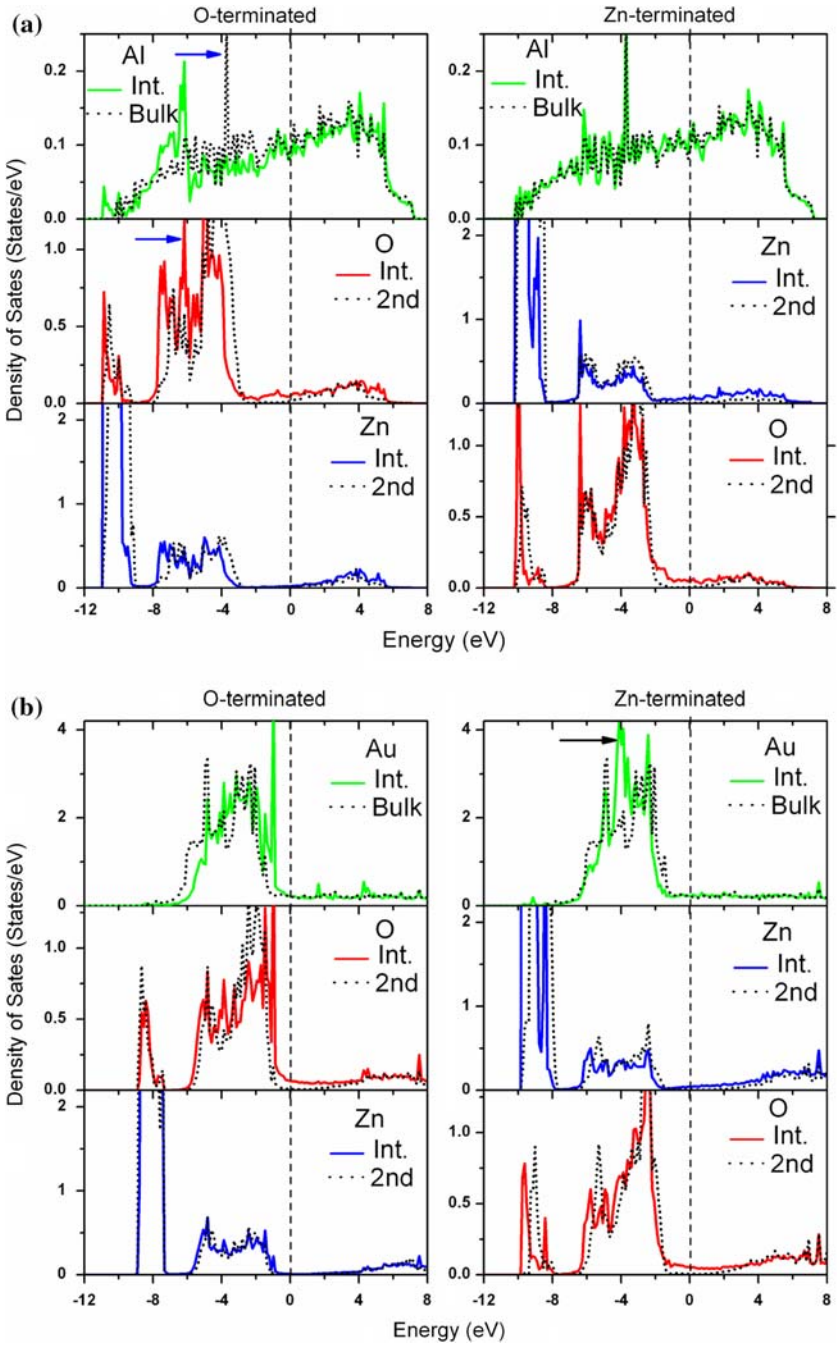

Fig. 3. PDOS for atoms in Al- (a) and Au-ZnO (b) interfaces. Each includes O- (left) and Zn-terminated (right) interface configurations. The Fermi level is at energy zero. In (a), new states appear at 6.3 eV below E_F at O-terminated ZnO due to Al-O bonding in both the Al and O interface layer DOS. In (b), new states appear at 4.1 eV below E_F at Zn-terminated ZnO due to Au-Zn bonding in both the Au and Zn interface layer DOS.

supercell, an electric field arises across the ZnO, as shown in Fig. 4. For the double-averaged potential (black solid line), there is a potential drop from the O- to Zn-terminated interface, across the ZnO due to the internal electrical field, while the potential within the metal is flat. One way to make Eq. 1 effective is to linearly extrapolate the double-averaged potential to the two interface planes, as shown by the dotted line in Fig. 4, where the values are taken as the reference levels.[27] Once the reference levels at the two interfaces are determined, the valence band edge (E_V) can be determined using the known Δ, which is a constant and derived from the ZnO bulk calculation. This procedure is shown in Fig. 4. Note that in ZnO, the energy difference between the double-averaged potential ($\bar{V}$, dotted line) and the valence band energy (E_V, dash-dotted line) is a constant (Δ), a bulk property of wurtzite

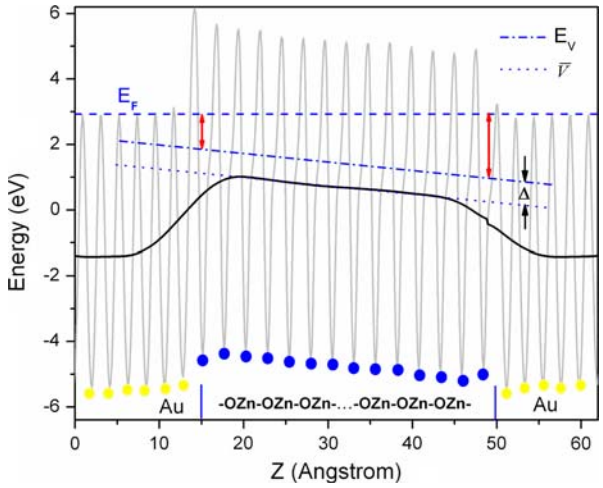

Fig. 4. Procedure to determine the barriers, $E_F - E_V$, at the two interface planes in the Au/ZnO interface supercell. In-plane averaged potential (grey curve, along the interface normal Z), double averaged potential (black solid line), valence band edge (E_V, dash-dotted line) and the Fermi level (E_F, dashed line) are shown. The linear extrapolation of the double averaged potential (black solid line) for ZnO is shown by the dotted straight line.

ZnO. The barriers, $E_F - E_V$, at the two interfaces, are shown by the double arrows. One may wonder whether the SBH generated in this way may be related to the length scale of the supercell. Actually, the strength of the internal electric field is reciprocal to the length of ZnO in the supercell and diminishes to zero for infinite ZnO. However, the potential drop from one interface to another across the ZnO is a constant and only depends on the boundary conditions. This means that the conserved property of the system is the SBH. We checked the SBH conservation by varying the length of ZnO. Interface supercells with 14 or 18 double-layers of ZnO were considered, with the same interface configurations. The SBH changes little (less than 0.1 eV), which clarify the correctness of the procedure to estimate the SBH.

Table III summarizes the calculated SBHs for various metal (Al, Ag, and Au)/ZnO interface configurations. These values are evaluated from the calculations of six interface supercells. Each one consists of an oxygen-terminated (on-top) interface and a Zn-terminated interface (either fcc or hcp hollow). Using the calculated band gap, the SBHs for O- (Zn-)terminated Al/ZnO, Ag/ZnO, and Au/ZnO interfaces are –0.6 eV (–0.3 to –0.1 eV), 1.0 eV (–0.2 eV), and 0.7 eV (–0.2–0.1 eV), respectively. The results show that SBHs at metal/ZnO interfaces are very sensitive to the specific interface chemical bonding. For the simple metal Al, the SBHs are negative for all interface configurations, which means that Ohmic contacts form at both polar interfaces. This is consistent with experimental results. The noble metals Ag and Au can both be used as electrodes for Schottky contacts. However, we found here that only Ag- or Au-oxygen interface bonds give Schottky contacts with high SBH (1.0 eV and 0.7 eV, respectively). Once metal-zinc bonds form at the interface, the SBH decreases sharply and the Fermi level is pushed close to the conduction band edge of ZnO or even into the conduction band. This may explain why Au- and Ag-ZnO Schottky contacts formed at room temperature are not stable and even become Ohmic under annealing, which may be due to the formation of interface metal-Zn bonds, for example, a Au-Zn eutectic.[28] From a more general point of view, we would say that interface metal-zinc bonds can give an interface Fermi level near the conduction band edge of ZnO, while the contribution of metal-oxygen bonds depends on the specific metal. Interface reactive metal-anion bonds (e.g., Al-O) tend to give Ohmic contacts while noble metal and cation bonding (e.g., Au-O or Ag-O) can form Schottky contacts.

Table III. Schottky Barrier Heights ($\Phi_B = E_C - E_F$, in eV) for Various Metal/ZnO Interfaces

Structures	Al/ZnO	Ag/ZnO	Au/ZnO
O-on-top	–0.6	1.0	0.7
Zn-hcp-hollow	–0.3	–0.2	–0.2
Zn-fcc-hollow	–0.1	–0.2	0.1

We should discuss the applicability and potential accuracy of our calculation here. First principles studies based on DFT have been widely used to calculate barrier heights at metal/compound semiconductor interfaces.[25] It is recognized that the absolute values of the calculated barrier heights could be different from experimental results because of the well-known problem of DFT in underestimating band gaps, especially for wide-band-gap semiconductors or insulators. However, the DFT calculations accurately describe the ground states of the interface systems and the relative values corresponding to different interface structures are always well obtained, as demonstrated in many calculations for metal/SiC and metal/high-K oxide interfaces.[13,14,29,30] We should note that the ideal surfaces considered in this study are different from as-received or chemically treated ZnO surfaces. Experimentally, it was found that the Zn-polar face has a slightly higher barrier height than the O-polar face.[31,32] This may be due to effects of interfacial oxide layers and/or high surface defect states, which may pin the interface Fermi level and overwhelm the effects of interface chemical bonding.

CONCLUSIONS

In conclusion, we present first-principles calculations based on density functional theory (DFT) of model metal/ZnO. Self-interaction corrections (GGA + U) were applied to widen the intrinsic-underestimated band gap of ZnO in GGA. The

atomic and electronic structures for a variety of metal/ZnO interfaces have been calculated. SBHs were evaluated in the presence of an internal uniform electric field. The results show that SBHs at metal/ZnO interfaces are very sensitive to the specific interface chemical bonding. Interfacial metal-zinc bonds tend to give Ohmic contacts, while the contribution of metal-oxygen bonds depends on the specific metal: reactive metals give Ohmic contact whereas noble metals give Schottky-like behavior. These results are in good agreement with experiments and emphasize the importance of interface chemical bonding on macroscopic metal/ZnO barriers that are likely to occur in conventional contact formation. Note that experimental measurements typically show that Schottky barrier heights for metals on ZnO crystalline surfaces increase with increasing work functions—as expected from a classical Schottky–Mott model as well as for metal-induced gap state models for relatively ionic semiconductors with only minor dielectric screening. This trend is common to most semiconductors and its sensitivity to work function can be strongly impacted by extrinsic effects. Our results show that the dipole due to local metal-ZnO chemical bonding can introduce an additional perturbation to this Schottky barrier versus work function dependence.

ACKNOWLEDGEMENT

The authors gratefully acknowledge Dr. Yuanping Feng at the National University of Singapore for the computation resources. We acknowledge Office of Naval Research Grant N00014-03-1-0001 (Colin Wood) for support of oxide electronic materials studies.

REFERENCES

1. S.J. Pearton, D.P. Norton, K. Ip, Y.W. Heo, and T. Steiner, *Prog. Mater. Sci.* 50, 312 (2005).
2. B.J. Coppa, R.F. Davis, and R.J. Nemanich, *Appl. Phys. Lett.* 82, 400 (2003).
3. H.L. Mosbacker, Y.M. Strzhemechny, B.D. White, P.E. Smith, D.C. Look, D.C. Reynolds, C.W. Litton, and L.J. Brillson, *Appl. Phys. Lett.* 87, 012102 (2005).
4. M.W. Allen, M.M. Alkaisi, and S.M. Durbin, *Appl. Phys. Lett.* 89, 103520 (2006).
5. K. Ip, G.T. Thaler, H. Yang, S.Y. Han, Y. Li, D.P. Norton, S.J. Pearton, S. Jang, and F. Ren, *J. Cryst. Growth* 287, 149 (2006).
6. L.J. Brillson, H.L. Mosbacker, M.J. Hetzer, Y. Strzhemechny, G.H. Jessen, D.C. Look, G. Cantwell, J. Zhang, and J.J. Song, *Appl. Phys. Lett.* 90, 102116 (2007).
7. S.B. Zhang, S.-H. Wei, and A. Zunger, *Phys. Rev. B* 63, 075205 (2001).
8. C.F. Brucker and L.J. Brillson, *Appl. Phys. Lett.* 39, 67 (1981).
9. L.J. Brillson, C.F. Brucker, A.D. Katnani, N.G. Stoffel, and G. Margaritondo, *Appl. Phys. Lett.* 38, 784 (1981).
10. L.J. Brillson, *Surf. Sci. Rep.* 2, 123 (1982).
11. R.T. Tung, *Phys. Rev. B* 64, 205310 (2001).
12. D.A. Ricci, T. Miller, and T.-C. Chiang, *Phys. Rev. Lett.* 93, 136801 (2004).
13. Y.F. Dong, Y.Y. Mi, Y.P. Feng, A.C.H. Huan, and S.J. Wang, *Appl. Phys. Lett.* 89, 122115 (2006).
14. A.A. Demkov, *Phys. Rev. B* 74, 085310 (2006).
15. B. Meyer and D. Marx, *Phys. Rev. B* 69, 235420 (2004).
16. A. Zaoui, *Phys. Rev. B* 69, 115403 (2004).
17. Z. Lin and P.D. Bristowe, *Phys. Rev. B* 75, 205423 (2007).
18. G. Kresse and J. Hafner, *Phys. Rev. B* 47, R558 (1993); G. Kresse and J. Hafner, *Phys. Rev. B* 48, 13115 (1993).
19. P.E. Blöchl, *Phys. Rev. B* 50, 17953 (1994); G. Kresse and J. Joubert, *Phys. Rev. B* 59, 1758 (1999).
20. S.L. Dudarev, G.A. Botton, S.Y. Savrasov, C.J. Humphreys, and A.P. Sutton, *Phys. Rev. B* 57, 1505 (1998).
21. A. Janotti, D. Segev, and C.G. Van de Walle, *Phys. Rev. B* 74, 045202 (2006).
22. P. Erhart, K. Albe, and A. Klein, *Phys. Rev. B* 73, 205203 (2006).
23. H.B. Michaelson, *J. Appl. Phys.* 48, 4729 (1977).
24. C.G. Van de Walle and R.M. Martin, *Phys. Rev. B* 34, 5621 (1986).
25. M. Peressi, N. Binggeli, and A. Baldereschi, *J. Phys. D* 31, 1273 (1998).
26. S.H. Wei and A. Zunger, *Phys. Rev. Lett.* 59, 144 (1987).
27. S. Picozzi, G. Profeta, A. Continenza, S. Massidda, and A.J. Freeman, *Phys. Rev. B* 65, 165316 (2002).
28. E.A. Brandes (ed.), *Smithells Metals Reference Book* (Buttersworth, London, 1983), pp. 11–94.
29. S. Tanaka and M. Kohyama, *Appl. Surf. Sci.* 216, 417 (2003).
30. L.R. Fonseca and A.A. Knizhnik, *Phys. Rev. B* 74, 195304 (2006).
31. H. Endo, M. Sugibuchi, K. Takahashi, S. Goto, S. Sugimura, K. Hane, and Y. Kashiwaba, *Appl. Phys. Lett.* 90, 121906 (2007).
32. M.W. Allen, P. Miller, R.J. Reeves, and S.M. Durbin, *Appl. Phys. Lett.* 90, 062104 (2007).